frontiers in Marine Science

ORIGINAL RESEARCH
published: 11 March 2022
doi: 10.3389/fmars.2022.824617

Influences of the 1855 AD Huanghe (Yellow River) Relocation on Sedimentary Organic Carbon Burial in the Southern Yellow Sea

Jianying Liu[1], Da-Wei Li[1,2], Yang Ding[1], Tiantian Ge[1], Weifang Chen[3], Chih-An Huh[4†] and Meixun Zhao[1,2]**

[1] *Frontiers Science Center for Deep Ocean Multispheres and Earth System, and Key Laboratory of Marine Chemistry Theory and Technology, Ministry of Education, Ocean University of China, Qingdao, China,* [2] *Laboratory for Marine Ecology and Environmental Science, Qingdao National Laboratory for Marine Science and Technology, Qingdao, China,* [3] *State Key Laboratory of Marine Environmental Science, College of Ocean and Earth Science, Xiamen University, Xiamen, China,* [4] *Institute of Earth Sciences, Academia Sinica, Nankang, Taipei, Taiwan*

OPEN ACCESS

Edited by:
Ying Wu,
East China Normal University, China

Reviewed by:
Siyuan Ye,
Qingdao Institute of Marine Geology (QIMG), China
Ding He,
Hong Kong University of Science and Technology, Hong Kong SAR, China

***Correspondence:**
Da-Wei Li
ldw@ouc.edu.cn
Meixun Zhao
maxzhao@ouc.edu.cn

[†] *Deceased*

Specialty section:
This article was submitted to Marine Biogeochemistry, a section of the journal Frontiers in Marine Science

Received: *29 November 2021*
Accepted: *21 February 2022*
Published: *11 March 2022*

Citation:
Liu J, Li D-W, Ding Y, Ge T, Chen W, Huh C-A and Zhao M (2022) Influences of the 1855 AD Huanghe (Yellow River) Relocation on Sedimentary Organic Carbon Burial in the Southern Yellow Sea. Front. Mar. Sci. 9:824617. doi: 10.3389/fmars.2022.824617

The Huanghe (Yellow River) supplies large amount of sediments and terrestrial organic carbon (OC) to the eastern Chinese marginal seas. A relocation of the Huanghe outlet from the southern Yellow Sea (YS) to the Bohai Sea occurred in 1855 AD, however, detailed knowledge about the impact of this relocation on sedimentary source and OC burial in Chinese marginal seas is still critically lacking. In this study, we present total OC content and its isotope ($\delta^{13}C$), along with bulk total organic carbon (TOC)/total nitrogen (TN) molar ratio and lipid biomarker contents, in a sediment core HH12 from the southern YS with sediment age spanning the last 300 years. We find that TOC and terrestrial lipid biomarker mass accumulation rates were lower between 1855 AD and 1950 AD than that prior to 1855 AD in core HH12; and in accordance, both TOC/TN ratio and $\delta^{13}C$ records indicate a gradual decrease of terrigenous source contributions to sedimentary OC. This suggests that the relocation of the Huanghe outlet reduced the transport of terrestrial OC to the southern YS. However, the $\delta^{13}C$ record also indicates a relative increase of terrestrial OC contribution to sedimentary OC after 1950 AD, and the most likely explanation is increased contributions from the old Huanghe delta erosion and Korean rivers. Future studies should focus on better constraining the variations of terrestrial and marine endmembers with $\delta^{13}C$ and $\Delta^{14}C$ analyses of specific biomarkers to examine these linkages.

Keywords: southern Yellow Sea, sedimentary organic carbon, 1855 AD, Huanghe outlet relocation, carbon isotopes, lipid biomarkers

INTRODUCTION

Accounting for more than 80% of annual global marine sediment organic carbon (OC) burial (Burdige, 2005), marginal seas play an important role in removing carbon from the active biosphere to the inactive geosphere. Marginal sea sedimentary OC is comprised of in situ-produced marine OC and terrestrial OC (Blair and Aller, 2012), which is a highly dynamic component of the carbon cycle (Bauer et al., 2013). The majority of terrestrial OC buried in marginal seas is delivered by rivers. The global river particulate organic carbon (POC) flux is ~200 million ton per year (Mt yr^{-1})

(Galy et al., 2015), and one-third of this OC escapes oxidation and is buried in continental margin sediments (Burdige, 2005). However, OC burial is environment-specific, especially in marginal seas receiving divergent river inputs and with distinctive environmental factors, thus detailed mechanisms controlling OC burial in marginal seas have remained elusive.

The eastern Chinese marginal seas include the Bohai Sea (BS), the Yellow Sea (YS) and the East China Sea (ECS) and accounts for ∼10% of global OC burial on continental margins (Burdige, 2005; Jiao et al., 2018). Given the spatially heterogeneous nature in terms of OC sources, the eastern Chinese marginal seas are hot spots in OC cycle research and have been well studied for the sources, transport processes and burial efficiency in surface sediments (Li et al., 2012; Yu et al., 2021; Zhao et al., 2021). The Huanghe (Yellow River) is the second largest river in China, with a drainage area of 7.45×10^5 km^2. It deliveries 0.34-0.58 Mt POC per year, and serves as the dominant source of terrestrial OC buried in the BS and the YS (Bao et al., 2018; Yu et al., 2021). During the past 2000 years, Huanghe changed its lower course for more than 20 times (Fan et al., 2019; He et al., 2019), and the last large-scale relocation took place in 1855 AD (**Figure 1**) as its outlet shifted to BS from the southern YS. Accompanied with the outlet relocations, the amount of Huanghe sediment discharged into the eastern Chinese marginal seas also changed significantly. From 1128 AD to 1546 AD, the lower Huanghe course bifurcated into several tributaries and most of the fluvial sediment was deposited on the pan-flood plain lies between southwest Shandong and Henan provinces (**Figure 1**) (Ren, 1992). Since 1578 AD, dikes were built to cut off the northeast flow in Shandong province and the Huanghe was fixed to capture the Huai River course draining into the southern YS, which ensured continuous input of the Huanghe sediment into the southern YS from 1578 AD to 1855 AD. During this period, the sediment discharge of the Huanghe increased to ∼1560 Mt yr^{-1} (Wu et al., 2020). After the Huanghe outlet transferred from the southern YS to the BS in 1855 AD, the sediment discharge remained ∼1310 Mt yr^{-1} for nearly 100 years (Wu et al., 2020). Since the late 1950s, the sediment yield from the Huanghe has experienced a dramatic decline to 150 Mt yr^{-1} in 2000s (Wang et al., 2011).

In response to this 1855 AD Huanghe relocation, significant changes of sedimentological properties and benthic ecosystem dynamics have been observed in the eastern Chinese marginal seas. For example, detailed geochemical element analysis was performed on sediment cores from the northern YS (Zhou et al., 2013) and the ECS (Yang et al., 2009), which revealed that trace metal elements decreased significantly in both regions after 1855 AD. Liao et al. (2015) have reported that the 1855 AD Huanghe relocation led to the decrease of grain size in the BS due to increased contribution of finer sediments from the Huanghe, and its sediment oxygenation changed from oxidation to weak oxidation-reduction state after 1855 AD. In the southern YS, benthic foraminifera abundance and species diversity increased after 1855 AD, with the dominant benthic foraminifera species changed from euryhaline and aktological cold water species to stenohaline cold water species (Fan et al., 2019). Zhou X. et al., 2014 provided evidence for the effect of 1855 AD Huanghe relocation on OC burial in the southern YS. total organic carbon (TOC)/total nitrogen (TN) ratio from site 35009 (**Figure 1**) was obviously lower after 1855 AD than pro to, indicating the proportion of terrestrial OC decreased significantly in the central southern YS. Using stable isotopes (δ^{13}C, δ^{15}N) and TOC/TN ratio, Yang et al. (2009) proposed that terrestrial OC proportion significantly reduced in the southwestern Cheju Island mud (SWCIM) after the Huanghe course shifted to the BS in 1855 AD.

However, impacts of the 1855 AD Huanghe relocation on OC burial in the eastern Chinese marginal seas have not been explored in detail, and significant gaps still remain with respect to the influences of this event on the OC sources, burial flux and controlling mechanisms. In this study, sediment contents of TOC, TN and terrestrial lipid biomarkers, and the δ^{13}C value of bulk sedimentary OC were measured in a sediment core HH12 from the southern YS spanning the past 300 years in an effort to quantify temporal variations of terrestrial OC burial. Results of this study provide insights to evaluate influences of the 1855 AD Huanghe relocation on sedimentary OC burial in the southern YS.

MATERIALS AND METHODS

Study Area and Sediment Core

The southern YS, locates between the mainland China and the Korean peninsula, is a semi-enclosed marginal sea with an average water depth of ∼44 m (Li et al., 2021; **Figure 1**). The major surface currents in the southern YS are the Yellow Sea Warm Current (YSWC) and coastal currents, i.e., the Korean Coastal Current (KCC) along the Korean Peninsula and the Yellow Sea Coastal Current (YSCC) along the Shandong Peninsula and the Jiangsu coast (Zang et al., 2003), prevailing in winter and spring seasons (Liu et al., 2013; **Figure 1**). Strong northwest wind drives the KCC and YSCC flow southward (Beardsley et al., 1983); to compensate the coastal current transport, the northward warm current, i.e., the YSWC, flows along the western slope of the south YS trough (Lin et al., 2011; Li et al., 2021). There are also strong tidal currents in the near shore region along the Jiangsu coast and Changjiang estuary, with the strongest tidal current speed > 150 cm s^{-1} (Bian et al., 2013). Tidal and wind-generated currents can induce strong bottom stresses which control the resuspension and deposition of sediments, therefore determining the transport of terrestrial sediment and the formation of muds.

Sediment core HH12 (35.00°N, 123.50°E, water depth 77 m; 48 cm long) was collected using a box-core sampler during the China Ocean Carbon (CHOICE-C I) Cruise I on the R/V Dongfanghong II in 2009 from the central southern YS mud (CSYSM, **Figure 1**). The sediments were sampled at 2 cm increments on board, with a portion used for dry bulk density analysis and remainders were stored at −20°C immediately.

Analytical Methods

^{210}Pb and ^{137}Cs

Sediment dating was by the gamma-spectrometry ^{210}Pb and ^{137}Cs method (Huh and Su, 1999). After collection, sediment

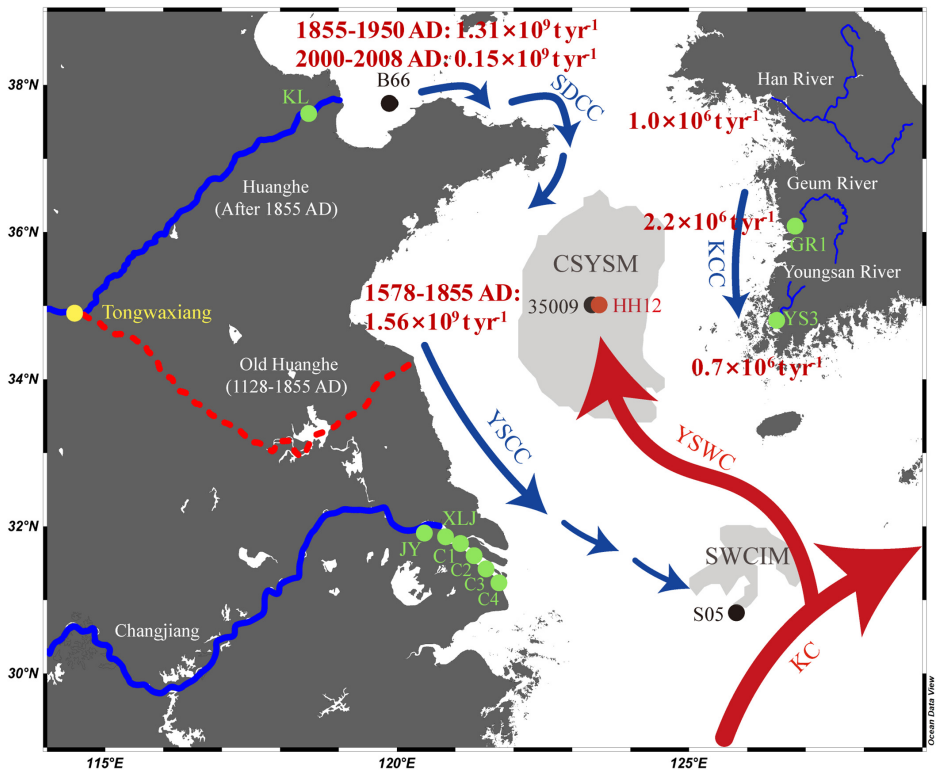

FIGURE 1 | Locations of core HH12 (●) and other core sites (●) referred in this study (35009, Zhou X. et al., 2014; B66, Xiao et al., 2020; S05, Yang et al., 2009). The green solid dots (●) represent river hydrological stations or sampling sites (KL, Yu et al., 2019a; XJY, JY, Wu et al., 2018; C1, C3, C5, C7, Sun et al., 2021; GR1, Kang et al., 2019; YS3, Lee et al., 2013) mentioned in this study. KL: kenli; XJY: xuliujing; JY: jiangyin. Sampling sites from the lower reach of the Han River is not shown because detail information was not reported by Yoon et al. (2016). The yellow solid dot (●) represents Tongwaxiang where the Huanghe changed its course at 1855 AD. The gray areas represent Central South Yellow Sea Mud (CSYSM) and Southwestern Cheju Island Mud (SWCIM) redrawn from Li G. et al. (2014). The currents (indicated by arrows) include: KC, Kuroshio Current; YSWC, Yellow Sea Warm Current; YSCC, Yellow Sea Coastal Current; SDCC, Shandong Coastal Current; KCC, Korean Coastal Current. River sediment discharge was labeled in red. Sediment discharge from the Huanghe was 1.56 × 10^9 t yr^{-1} during 1578-1855 AD (Wu et al., 2020), 1.31 × 10^9 t yr^{-1} during 1855-1950 AD (Wang et al., 2011) and 0.15 × 10^9 t yr^{-1} 2000-2008 AD (Wang et al., 2011). Sediment discharges from Han River, Geum River and Youngsan River were 1.6 × 10^6 t yr^{-1}, 2.2 × 10^6 t yr^{-1} and 0.7 × 10^6 t yr^{-1}, respectively (Qiao et al., 2017).

samples were dried, weighed, and stored in the sealed plastic vessels. These samples were left at least for 2 weeks in order to establish radioactive equilibrium between ^{226}Ra and ^{222}Rn. Then specific gamma rays of ^{210}Pb (46.52 keV), ^{214}Pb (351.99 keV) and ^{137}Cs (661.6 keV) were measured using the HPGe detectors: GMX-type (ORTEC GMX-120265) and LoAX-type (ORTEC LoAX-70450) at Academia Sinica (Taiwan). The details about the performance and the calibration of these detectors have been described in Huh et al. (2011). The counting time for each sample varied from a few hours to a few days.

^{214}Pb was used as an index of supported ^{210}Pb whose activity concentration was subtracted from that of the measured, total ^{210}Pb to obtain excess ^{210}Pb ($^{210}Pb_{ex}$):

$$^{210}Pb_{ex} = {}^{210}Pb - {}^{214}Pb \quad (1)$$

To derive ^{210}Pb-based rates, semi-log plots were used and showed in **Figure 2A**. From the slope (m) of $^{210}Pb_{ex}$ decrease (decay) down core, assuming a constant initial concentration of the radionuclide, sedimentation rate (SR_{Pb-210}) is calculated by SR_{Pb-210} = -λ/m, where λ is the decay constant of ^{210}Pb. ^{137}Cs, with a half-life of 30 years, has been emitted to the environment due to the nuclear weapon testing. Because the maximum fallout of ^{137}Cs occurred in 1963 AD (Ritchie and McHenry, 1990), the ^{137}Cs can provide an independent check to validate ^{210}Pb chronology (Smith, 2001; Lu, 2004; Lu and Matsumoto, 2005).

Dry Bulk Density

The sediment dry bulk density (DBD) was measured by ring-knife. A clean and dry ring knife (mass M, volume V) was filled with fresh sediment, and then was freeze-dried at −60°C and weighted (M_{total}). DBD was calculated as follows:

$$DBD(gcm^{-3}) = (M_{total} - M)/V \quad (2)$$

Mass accumulation rate (MAR) for TOC, TN and lipid biomarkers were calculated as follows:

$$MAR_C = [C] \times SR \times DBD \quad (3)$$

Where [C] is the biomarker (or OC, TN) content and SR (cm yr^{-1}) is the sedimentation rate.

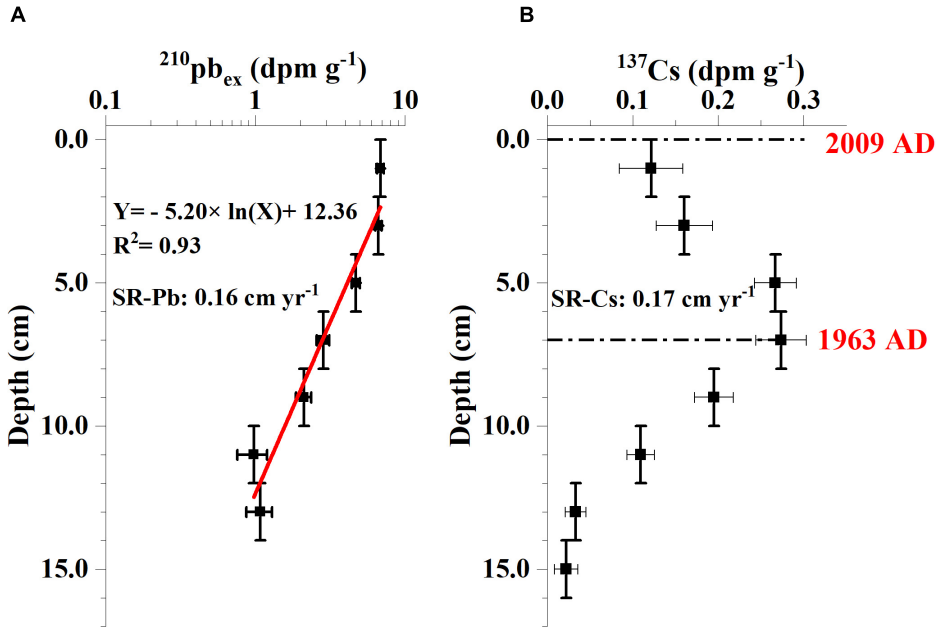

FIGURE 2 | (A) Downcore profiles of ln ($^{210}Pb_{ex}$) and **(B)** ^{137}Cs activities in core HH12.

Organic Carbon and Total Nitrogen

Freeze-dried sedimentary samples of ∼1 g were rinsed with 6 M HCl (12 h at room temperature) to remove carbonate. After rinsing four times with deionized water to remove HCl and drying in an oven at 55°C for 48 h, 5–30 mg of the carbonate-free sediment sample was then analyzed for TOC and TN contents with an Elemental Analyzer FLASH 2000 at Ocean University of China. The TOC and TN accuracy was determined by replicate analysis of atropine (Thermo Fisher Scientific, Netherlands) and a low-organic content soil (Elemental Microanalysis Ltd., United Kingdom), with a standard deviation of ± 0.02 wt% (n = 6) for TOC and ± 0.002 wt% for TN (n = 6), respectively.

Stable Isotope of Bulk Organic Carbon

Another 5–30 mg of the decarbonated sample was used to determine stable isotope of bulk organic carbon (TOC-$\delta^{13}C$) using Thermo Delta-V isotopic ratio mass spectrometer (the United States) (continuous-flow mode) at Ocean University of China. Measured $\delta^{13}C$ values were calibrated against USGS 40 ($\delta^{13}C$ = −26.39‰ vs. Vienna Pee Dee Belemnite, VPDB), IAEA-CH3 ($\delta^{13}C$ = −24.72‰ vs. VPDB) and IAEA 600 ($\delta^{13}C$ = −27.77‰ vs. VPDB) and a laboratory working standard ($\delta^{13}C$ = −23.8‰ vs. VPDB). The standard deviation of $\delta^{13}C$ measurement was less than ± 0.1‰ (n = 6) determined by the analyses of isotope standards.

Lipid Biomarkers

Lipid biomarkers were analyzed following the procedure described by Li D. et al. (2014). Briefly, freeze-dried sediment samples of ∼5 g were sonication-extracted (4 times) with organic solvent mixture (dichloromethane/methanol, v/v = 3:1) after adding C_{24} deuterium substituted n-alkane (n-$C_{24}D_{50}$) as internal standard. Total lipid extracts were concentrated under N_2 gas and further saponified with 6% KOH in methanol overnight and the neutral components were then extracted with n-hexane (4 times) and were further separated into apolar and polar fractions by silica gel chromatography *via* elution with n-hexane (8 ml) and dichloromethane/methanol (v/v = 95:5, 12 ml), respectively. For biomarker analyses, the aploar fraction which contains n-alkanes was injected into an Agilent 6890 N gas chromatograph (GC, the United States) equipped with a flame ionization detector (FID) and the HP-1 capillary column (50 m × 0.32 mm, 0.17 μm film thickness). The oven temperature program was as follows: 80°C for 1 min initially, increasing to 200°C at 25°C min^{-1}, then increasing to 250°C at 4°C min^{-1}, then increasing to 300°C at 1.6°C min^{-1} (holding for 12 min), and finally increasing to 320°C at 5°C min^{-1} (holding for 5 min). Quantification of lipid biomarkers was achieved by comparing GC-FID peak areas of target compound with that of the internal standard n-$C_{24}D_{50}$. In our laboratory, duplicate measurements resulted in a precision better than 10% and recovery of the extraction on biomarkers is >85% determined by replicate analyses on internal standards.

Potential Source Endmembers

Endmembers of $\delta^{13}C_{org}$, TOC/TN and OC content from river and marine OCs were used to distinguish OC sources to site HH12. Source endmembers were based on previous studies. The Huanghe $\delta^{13}C_{org}$ endmember of -24.0 ± 0.4‰ and 1/POC of 3.52 ± 1.85 were estimated from POC samples collected at the Kenli hydrographic station (37.61°N, 118.54°E; n = 13) closest to the modern Huanghe estuary in Dongying city (Tao et al., 2015; Yu et al., 2019a). The Changjiang $\delta^{13}C_{org}$ endmember of -26.4 ± 0.8‰ and 1/POC of 0.60 ± 0.44 were estimated from POC samples collected at Xuliujing (31.78°N, 120.93°E; n = 4) and Jiangyin (31.91°N, 120.26°E; n = 1) hydrographic stations

(Wu et al., 2018) and four sampling sites with salinity of 0 in the Changjiang estuary (C1, C3, C5, C7; n = 11; Sun et al., 2021). The $\delta^{13}C_{org}$ endmember of -27.2 ± 3.5‰ and 1/POC of 0.06 ± 0.05 for Geum River were estimated by POC collected from GR1 site (36.10°N, 126.87°E; n = 11; Kang et al., 2019). The $\delta^{13}C_{org}$ endmember of -22.2 ± 5.1‰ and 1/POC of 0.07 ± 0.05 for Youngsan River were constrained by POC samples collected from YS3 site (34.81°N, 126.54°E; n = 6) in the estuary (Lee et al., 2013). The $\delta^{13}C_{org}$ endmember of -23.9 ± 3.3‰ for Han River was constrained by POC samples (n = 16) collected in the lower reach of the Han River (Yoon et al., 2016) and there was no published available POC data in the lower of Han River. The marine OC endmember $\delta^{13}C$ value of -20.8 ± 0.8‰ was based on the global average for phytoplankton (Hedges et al., 1997; Blair and Aller, 2012) and the marine $1/C_{org}$ of 0.03 ± 0.03 was used (Kao et al., 2014).

The TOC/TN endmembers of 7.8 ± 2.2 (n = 6) for Huanghe and 7.6 ± 0.5 (n = 11) for Changjiang were constrained by POC samples collected at the Kenli hydrographic station (Yu et al., 2019a) and at sites C1, C3, C5, C7 in Changjiang estuary (Sun et al., 2021), respectively (**Figure 1**). The TOC/TN ratio endmembers of 13.0 ± 4.5 (n = 11) for Geum River, 5.9 ± 0.8 (n = 6) for Youngsan River and 6.7 ± 1.4 (n = 16) for Han River were constrained by POC samples collected at sites GR1 (Kang et al., 2019), YS3 (Lee et al., 2013) and the lower reach of the Han River (Yoon et al., 2016), respectively. The marine TOC/TN endmember value of 7.0 ± 1.0 was based on the average C/N ratio range of 6–8 of phytoplankton (Redfield et al., 1963; Müller, 1977).

RESULTS

Sediment Chronology

The average sedimentation rate of core HH12 was calculated as 0.16 cm yr^{-1}, which is similar to 0.15 cm yr^{-1} in core 35009 collected in the same site (35.00°N, 123.50°E, water depth 75.8 m; Zhou X. et al., 2014) as us basing on high resolution $^{210}Pb_{ex}$ and ^{137}Cs profiles, and is consistent with sedimentation rate of 0.1-0.2 cm yr^{-1} in the CSYSM (Qiao et al., 2017). The peak value (0.274 ± 0.029 dpm g^{-1}) of ^{137}Cs activity occurred at 6-8 cm in core HH12, corresponding to 1965 AD calculated by the $^{210}Pb_{ex}$ sedimentation rate (**Figure 2B**). In addition, by assuming constant sediment deposition through the top 7 cm, mean sedimentation rate obtained from ^{137}Cs profile is 0.17 cm yr^{-1}, which agrees well with the sedimentation rate from the ^{210}Pb method. By applying the mean sedimentation rate of 0.16 cm yr^{-1}, the age span of core HH12 was determined to be 300 years (1709-2009 AD). Because the ^{210}Pb dating method is applicable only for ∼150 years, the age uncertainties for the deeper sediments of core HH12 may be larger considering the potential changes of sedimentation rate in the southern YS due to the 1855 AD Huanghe relocation. However, it is reasonable to assume constant sedimentation rate after the 1855 AD Huanghe relocation, and this could have given reasonable sedimentation ages for the last 150 years. Therefore, this extrapolated age model can be used for the discussion on the 1855 AD Huanghe relocation event. Further support for this age model comes from regional studies which revealed significant changes of organic geochemical and mineral proxies around 1855 AD in the southern YS (Zhou X. et al., 2014) and the ECS (Yang et al., 2009) using extrapolate ^{210}Pb ages by assuming constant sedimentation rate (see discussion below).

Sedimentary Characteristics

The sediment DBD varied in the range of 0.54-0.81 g cm^{-3}. DBD was in a stable state between 1715-1853 AD (average: 0.74 g cm^{-3}), then decreased to 0.65 g cm^{-3} at 1865 AD, and increased to 0.81 g cm^{-3} in 1903 AD followed by a gradual decline to 0.54 g cm^{-3} at 2003 AD (**Figure 3A**). The sediment MAR varied in a range between 0.09 and 0.13 g cm^{-2} yr^{-1}, displaying similar pattern with DBD. Sediment MAR was 0.11-0.13 g cm^{-2} yr^{-1} (average: 0.12 g cm^{-2} yr^{-1}) during 1715-1903 AD except a low values of 0.10 g cm^{-2} yr^{-1} at 1865 year AD, and then it gradually decreased to 0.09 g cm^{-2} yr^{-1} at 2003 AD (**Figure 3B**).

Content and Mass Accumulation Rate of Total Organic Carbon and Total Nitrogen

Total organic carbon of core HH12 had been reported by Fan et al. (2014). The TOC contents varied within a narrow range of 0.38-0.67% (wt) (**Figure 3C**, purple) with the lowest value of 0.38% at 1803 AD. TOC was 0.56% on average (excluding the data from 1803 AD) between 1715AD and 1853 AD, then it decreased gradually to 0.44% at 1928 AD followed by a rapid increase to to 0.67% at the core top (2003 AD). Mass accumulation rates of TOC (TOC_{MAR}) varied in a relatively narrow range of 5.25-7.34 g m^{-2} yr^{-1} except one low value (4.33 g m^{-2} yr^{-1}) at 1803 AD (**Figure 3C**, red). Unlike TOC contents, TOC_{MAR} values were higher during 1715-1903 AD, and lower over the last 100 years.

The contents of TN (**Figure 3D**, brown) varied in a range of 0.05-0.11% (wt). TN content experienced a gradual increasing trend over the last 300 years except the lowest value of 0.05% at 1803 AD and lower values centered around 1928 AD. Mass accumulation rates of TN (TN_{MAR}) varied in a relatively narrow range of 0.75-1.20 g m^{-2} yr^{-1} except one low value (0.55 g m^{-2} yr^{-1}) at 1803 AD (**Figure 3D**, black). TN_{MAR} increased gradually from 0.75 g m^{-2} yr^{-1} at 1715 AD to 1.20 g m^{-2} yr^{-1} at 1890 AD, then it decreased to 0.91 g m^{-2} yr^{-1} at 1928 AD and keep stable over the last 70 years.

Content and Mass Accumulation Rate of Long-Chain n-Alkanes

Content of long chain n-alkanes was expressed in ng per g dry sediment (ng g^{-1}). Contents of the total long-chain n-alkanes (**Figure 4B**, purple), i.e., $\Sigma(C_{27} + C_{29} + C_{31})$, of core HH12 varied in the range between 190 and 410 ng g^{-1} (average: 253 ng g^{-1}). It displayed a stable trend from 1715 AD to 1853 AD, and a significant decrease from 1865 AD toward 1890 AD (average: 196 ng g^{-1}), then a slight increase to 246 ng g^{-1} at 1953 AD, and a rapid increase to 395 ng g^{-1} at 2003 AD (**Figure 4B**, purple). The

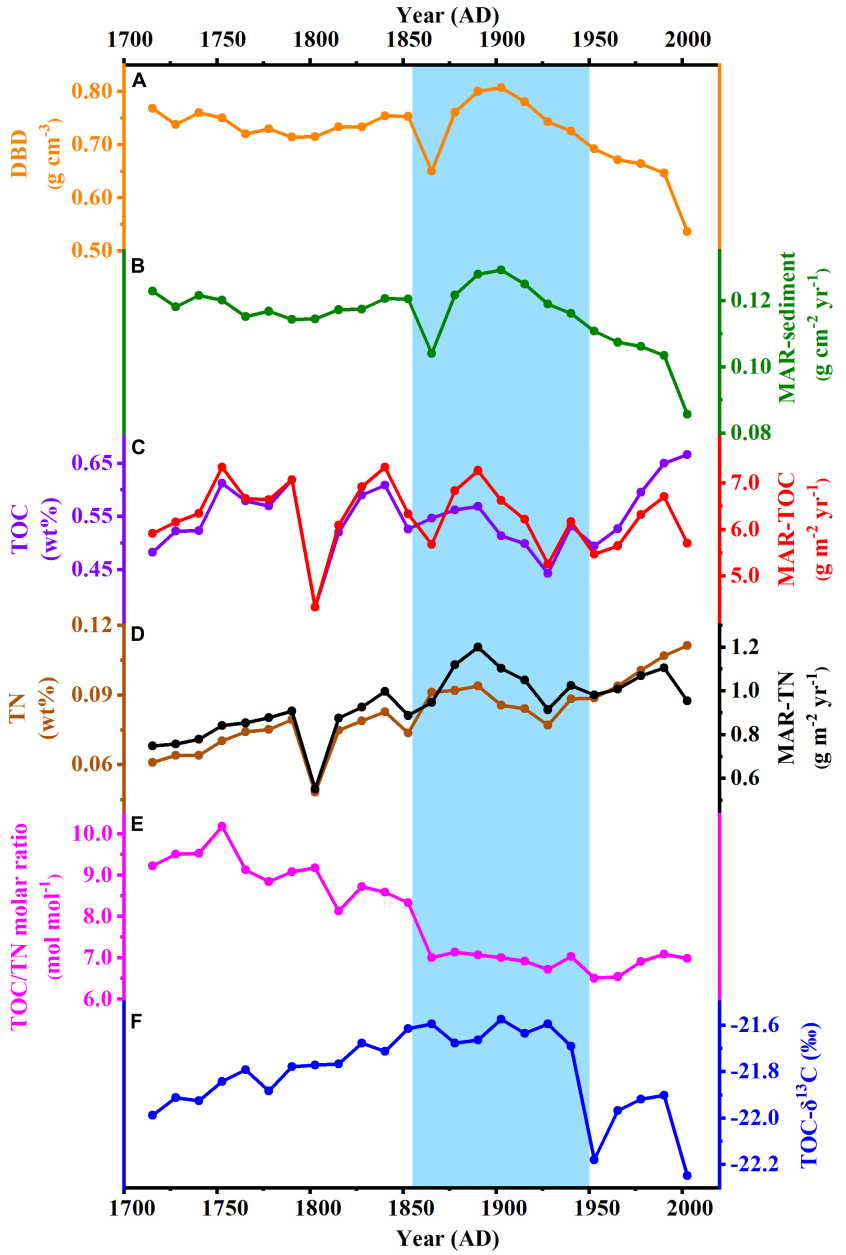

FIGURE 3 | Sedimentary records from core HH12 over the last 300 years. **(A)** Dry sediment bulk density (DBD). **(B)** Mass accumulation rate (MAR) of sediment. Sediment MAR is calculated as: $MAR_{sediment}$ = LSR × DBD. **(C)** Content (purple) and MAR (red) of TOC. **(D)** Content (brown) and MAR (black) of TN. **(E)** TOC/TN molar ratio. **(F)** Stable carbon isotope of bulk organic carbon (TOC-δ^{13}C).

MAR of $\Sigma(C_{27} + C_{29} + C_{31})$ of core HH12 ranged from 21 to 42 ng cm^{-2} yr^{-1} (average: 29 ng cm^{-2} yr^{-1}), showing a similar pattern with long-chain *n*-alkanes content (**Figure 4B**, black).

The Total Organic Carbon/Total Nitrogen Molar Ratio and δ^{13}C of Total Organic Carbon

The TOC/TN molar ratios of core HH12 varied in a range between 6.5 and 10.2 with the highest value of 10.2 at 1753 AD and the lowest value of 6.5 at 1953 AD. TOC/TN experienced a continuous decrease (from 9.2 to 7.0) from 1715 to 1865 AD and then a stable narrow range of 6.5-7.1 (mean: 6.9) from 1865 AD to 2003 AD (**Figure 3E**). TOC-δ^{13}C values in core HH12 varied between -22.2 and -21.6‰, with the most depleted values at 2003 AD (-22.2‰). TOC-δ^{13}C increased gradually from -22.0‰ at 1715 AD to -21.6‰ at 1853 AD, and kept relatively stable for nearly 100 years, then it decreased abruptly to -22.2‰ at 1953 AD, followed by low values between 1953-2003 AD (average: -22.0‰) (**Figure 3F**).

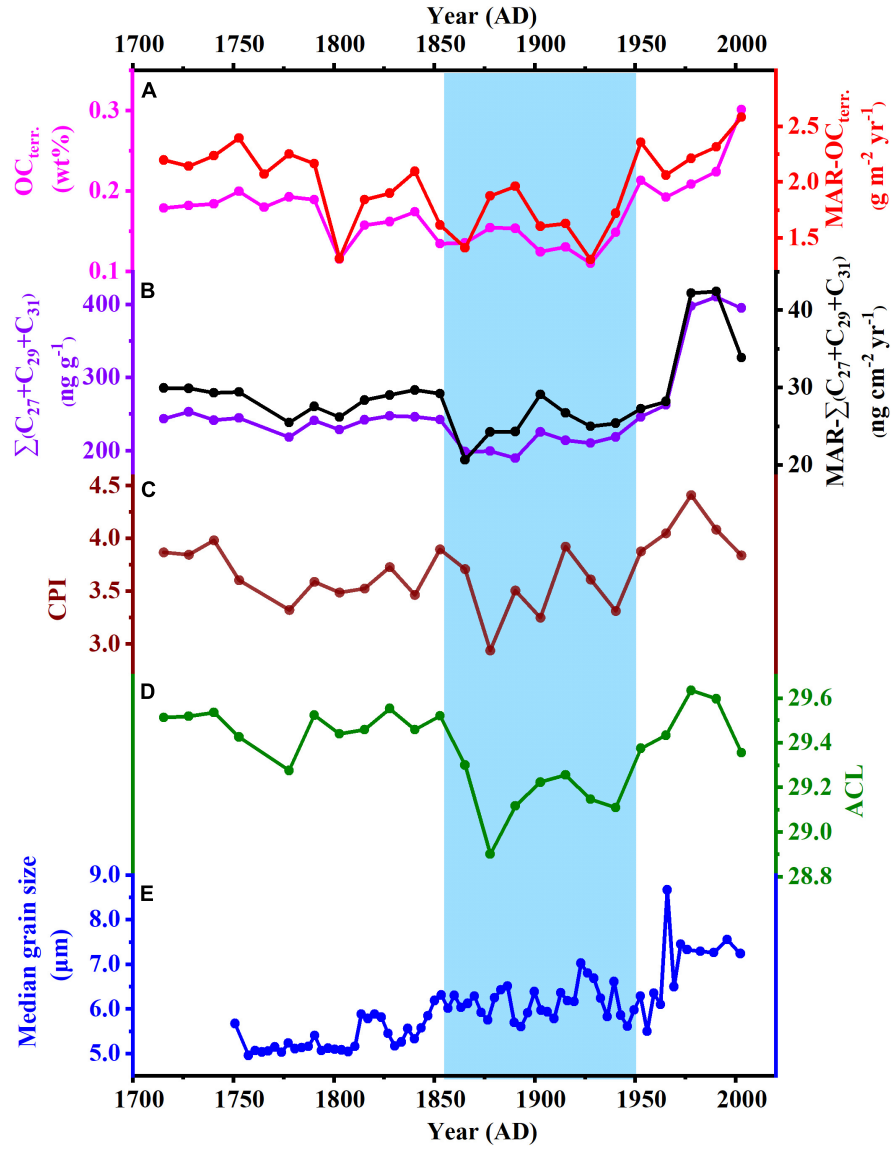

FIGURE 4 | Terrestrial OC records and *n*-alkanes indexes from core HH12 and median grain size from core 35009. **(A)** Content (pink) and mass accumulation rate (MAR) (red) of terrestrial OC calculated by TOC-$\delta^{13}C$ mixing model from core HH12 (this study). **(B)** Content (purple) and MAR (black) of Σ (C_{27} + C_{29} + C_{31}), i.e., sum of long chain of *n*-alkanes C_{27}, C_{29}, C_{31}, from core HH12 (this study). **(C)** Carbon preference index (CPI) from core HH12 (this study). CPI = 0.5 × (C_{25} + C_{27} + C_{29} + C_{31} + C_{33})/ (C_{24} + C_{26} + C_{28} + C_{30} + C_{32}) + 0.5 × (C_{25} + C_{27} + C_{29} + C_{31} + C_{33})/ (C_{26} + C_{28} + C_{30} + C_{32} + C_{34}). **(D)** Average chain length (ACL) from core HH12 (this study). ACL = (25 × C_{25} + 27 × C_{27} + 29 × C_{29} + 31 × C_{31} + 33 × C_{33})/ (C_{25} + C_{27} + C_{29} + C_{31} + C_{33}). **(E)** Median grain size from core 35009 (Zhou X. et al., 2014). Content of long chain *n*-alkanes was expressed in ng per g dry sediment (ng g^{-1}).

DISCUSSION

Organic Carbon Sources in the Southern Yellow Sea

Marginal sea sediments receive vast quantities of terrestrial OC and in situ-produced marine OC (Burdige, 2005; Blair and Aller, 2012). Today, the southern YS receives fluvial sediments from both Chinese rivers including the Huanghe and Changjiang (Yangtze River), and Korean rivers including Han, Geum and Youngsan rivers, thus terrestrial OC in the southern YS is complicated by different sources. Marine OC is characterized by C/N ratio (molar ratio is used in this study) of 6–8 (Redfield et al., 1963) and terrestrial OC is characterized by C/N ratio >20 (Meyers and Ishiwatari, 1993). Due to the existence of terrestrial inorganic N during the measurement process on bulk sediment N, TOC/TN ratio (molar ratio) has been used to distinguish sedimentary OC sources (Meyers, 1997; Calvert, 2004). Stable carbon isotope of total organic carbon provides another way to estimate sediment OC sources, with marine source OC characterized by $\delta^{13}C$ values range from

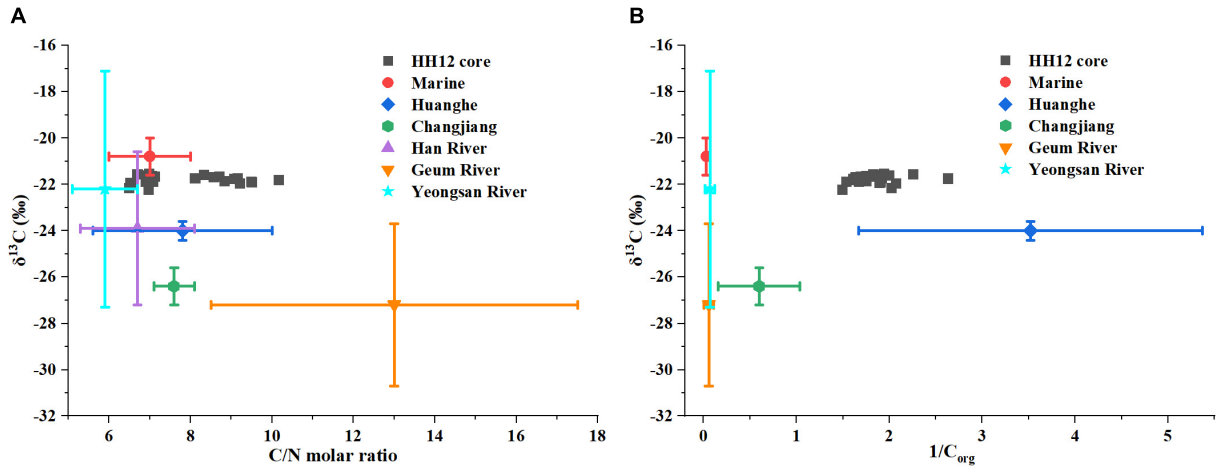

FIGURE 5 | Cross-plots of $\delta^{13}C$ versus C/N molar ratio **(A)** and $1/C_{org}$ **(B)**. Endmembers values used in this figure are as follows: POC-$\delta^{13}C$, $1/C_{org}$ and C/N endmembers of the modern Huanghe are from Tao et al. (2015) and Yu et al. (2019a); POC-$\delta^{13}C$, $1/C_{org}$ and C/N endmembers of the modern Changjiang are from Wu et al. (2018) and Sun et al. (2021). POC-$\delta^{13}C$, $1/C_{org}$ and C/N endmembers of the modern Geum River, Youngsan River and Han River are from Kang et al. (2019); Lee et al. (2013) and Yoon et al. (2016), respectively. POC-$\delta^{13}C$, $1/C_{org}$ and C/N endmembers of the marine source are from Redfield et al. (1963), Müller (1977), Hedges et al. (1997), Blair and Aller (2012), Kao et al. (2014).

−22 to −20‰ (O'Leary, 1988) and terrestrial OC from C_3 and C_4 plants characterized by $\delta^{13}C$ values range from −29 to −24‰ and −14 to −12‰ (Liu et al., 2005), respectively. Therefore, a plot of TOC/TN versus $\delta^{13}C$ can help to constrain OC sources in the southern YS because there exist large differences in both TOC/TN and $\delta^{13}C$ endmember values of OC delivered by these rivers (**Figure 5A**). In addition, large differences of OC content in river particles also exist among the rivers (**Figure 5B**) flowing into the BS and the YS, and thus a plot of the inverse of OC content and $\delta^{13}C$ can also provide constrain on OC sources in the southern YS.

As shown in **Figure 5A**, marine OC is characterized by more positive $\delta^{13}C$ value compared with that of rivers and our core sediments, thus both mixing scenarios between marine and Chinese rivers and between marine and Korean rivers can produce the TOC/TN and $\delta^{13}C$ values of core HH12 sediments. Marine endmember has the highest OC content value (i.e., lowest 1/OC, **Figure 5B**), however, due to the higher OC content of both Korean rivers and the Changjiang compared with that of core HH12 sediments, the mixing between marine OC and Huanghe derived terrestrial OC is the only scenario can produce the 1/OC and $\delta^{13}C$ values in core HH12 sediments. This suggests the Huanghe was the primary source of terrestrial OC to the southern YS. Further evidence supporting this comes from several previous studies. (1) Based on numerical clustering algorithm on bulk OC content and $\Delta^{14}C$, Van der Voort et al. (2018) proposed that terrestrial OC in southern YS sediment was mainly derived from the Huanghe. (2) By using Al-Mg regression analysis, Lim et al. (2020) proposed that detritus sediment in the western side of the southern YS was dominantly from Chinese rivers. (3) Sediment accumulation rate of the CSYSM was of 230 Mt yr^{-1} (Qiao et al., 2017), which far exceeded 6-20 Mt yr^{-1} of the sediment load in Korean rivers (Lim et al., 2007). (4) Although the southern YS lies close to the Changjiang estuary, the majority of Changjiang sediment and OC was deposited in the Changjiang estuary and the remainder was transported southward by coastal current depositing along the Zhejiang-fujian coastal (Liu et al., 2007; Wang et al., 2007; Yang et al., 2016).

Temporal Variations of Organic Carbon Composition in the Southern Yellow Sea From 1715 to 1950 AD

Sediment discharge from the Huanghe into eastern Chinese marginal seas experienced high level of 1560 Mt yr^{-1} during 1578-1855 AD (Wu et al., 2020), resulting in a rapid land growth at the speed of 11.1-21.8 km^2 yr^{-1} in Jiangsu coast during 1578-1855 AD (Zhang, 1984). After the lower Huanghe course shifted back to the BS in 1855 AD, the transport of Huanghe derived sediment to the southern YS experienced a long-distance by crossing the BS and northern YS. Meanwhile, the old Huanghe delta system in Jiangsu province changed from a prograding to a retrograding state and it suffered continuous erosion of 500-790 Mt yr^{-1} (Zhou L. et al., 2014). In response to these dramatic changes, we find obvious changes of terrestrial OC sources and burial in the southern YS.

Impact of the 1855 AD Huanghe Relocation on Organic Carbon Burial in the Southern Yellow Sea

The first evidence comes from the TOC/TN record in core HH12. The TOC/TN ratio decreased significantly from 8.1-10.2 prior to 1855 AD to 6.5-7.1 over the last 150 years (**Figure 6A**), suggesting decreased contribution of terrestrial OC to sedimentary OC in core HH12 after the Huanghe relocation. Taken together with a slightly decrease of TOC content and MAR (**Figure 3C**), this reveals that terrestrial OC burial flux (i.e., mass accumulation rate) decreased significantly since 1855 AD. Similar decreasing trends of TOC/TN ratio

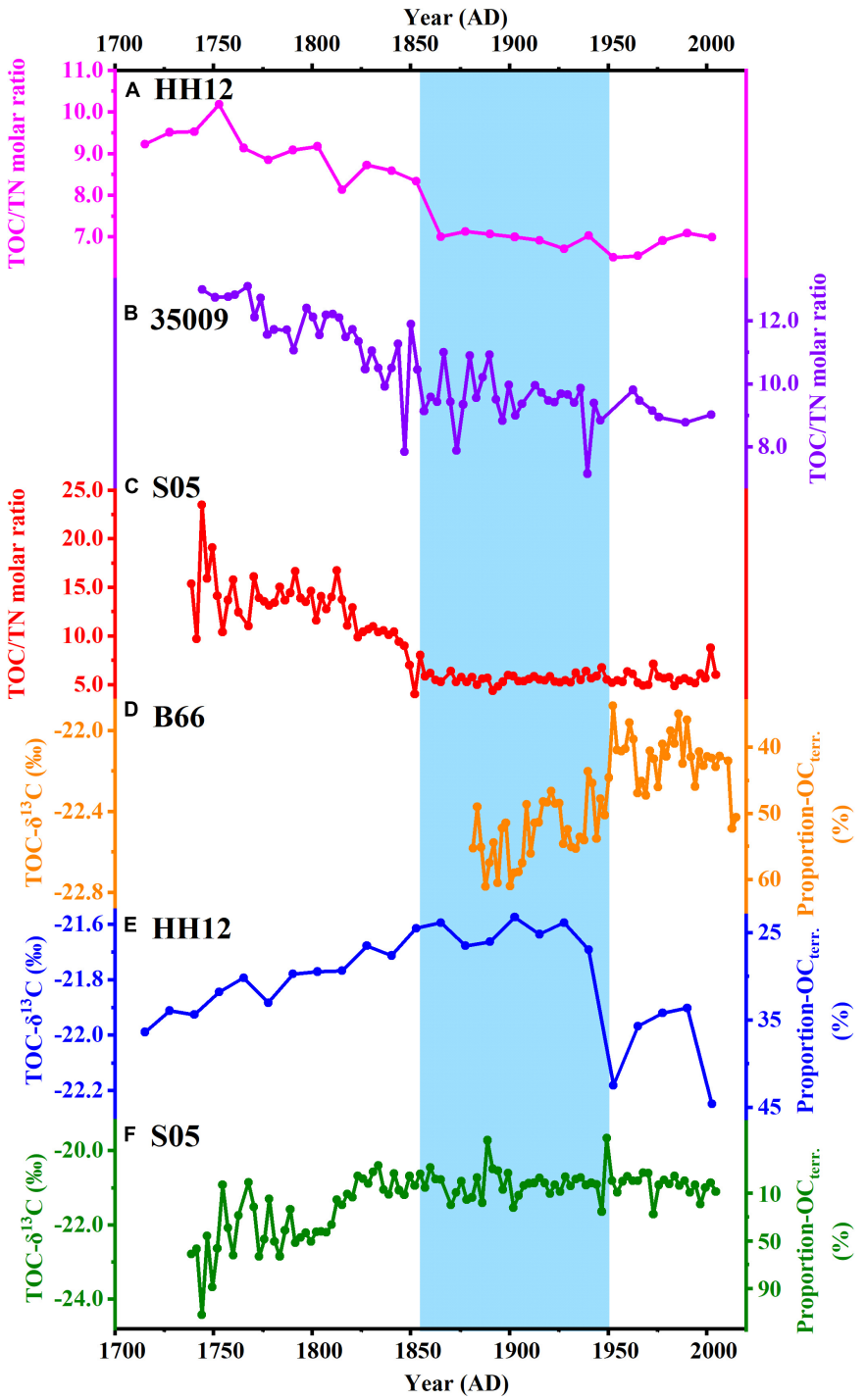

FIGURE 6 | The TOC/TN molar ratio and $\delta^{13}C_{TOC}$ from cores HH12, 35009, B66 and S05. **(A)** The TOC/TN molar ratio of core HH12 (this study). **(B)** The TOC/TN molar ratio of core 35009 (Zhou X. et al., 2014). **(C)** The TOC/TN molar ratio of core S05 (Yang et al., 2009). **(D)** The $\delta^{13}C$ of TOC of core B66 (Xiao et al., 2020). **(E)** The $\delta^{13}C$ of TOC of core HH12 (this study). **(F)** The $\delta^{13}C$ of TOC of core S05 (Yang et al., 2009). Proportions of terrestrial OC calculated using $\delta^{13}C$ binary mixing model were also labeled in **(D–F)** displayed on the right Y-axis of each panel.

(**Figures 6B,C**) around 1855 AD have been observed in core 35009 collected from the CSYSM (Zhou X. et al., 2014) and core S05 (30.85°N, 125.85°E) collected from the SWCIM (Yang et al., 2009), suggesting wide spread responses of reduced terrestrial OC burial in response to the 1855 AD Huanghe relocation. Due to the large uncertainty of terrestrial TOC/TN

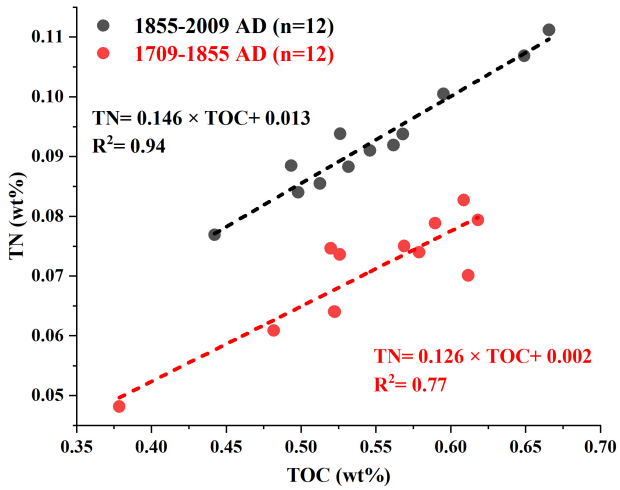

FIGURE 7 | Total nitrogen (TN) versus total organic carbon (TOC) in core HH12. Two data at 1728 AD and 1740 AD overlapped in this figure.

endmember, it has been reported that the TOC/TN ratio is not suitable to make quantitative calculation for the proportions of terrestrial and marine OCs in the southern YS (Xing et al., 2014; Yoon et al., 2016). A close linear correlation between TOC and TN suggests constant terrestrial and marine OC sources with changing proportions (Schubert and Calvert, 2001; Lamb et al., 2006). The linear correlation between TOC and TN has a significant positive intercept, suggesting the presence of total inorganic nitrogen (TIN) in sediment samples (Goñi et al., 1998; Schubert and Calvert, 2001), and the positive Y-intercept was considered as the content of TIN. However, in core HH12, the plot of TOC versus TN showed two different regression lines before and after 1855 AD (**Figure 7**). TOC/TN ratio showed higher values with low TN intercept between 1715-1855 AD, and lower values with high TN intercept over the last 150 years. The distinct variations of TIN suggest sediment sources to site HH12 changed around 1855 AD, in accordance, terrestrial OC source and composition to site HH12 should also have changed from terrestrial OCs contained more N-depleted to more N-enriched compounds.

The second evidence comes from the TOC-δ^{13}C record which provides another way to distinguish sediment OC sources. As shown in **Figure 3F**, the TOC-δ^{13}C of core HH12 increased from -22.0‰ at 1715 AD to -21.6‰ around 1855 AD, indicating a small decrease of terrestrial OC proportion. It is noteworthy that the TOC-δ^{13}C (and the TOC/TN) values increased (decreased) continuously from 1750 AD to 1855 AD. This suggests a transitional process prior to the 1855 AD Huanghe relocation event, which has also been observed on TOC-δ^{13}C and TOC/TN records from the southern YS (site 35009) and ECS (site S05). In contrast to TOC/TN record with abrupt change near 1855 AD, the TOC-δ^{13}C is stable around 1855 AD (**Figures 3E,F**). Start from the 1855 AD, TOC-δ^{13}C remained roughly stable at high values for about 100 years before decreased significantly to the range of -22.0 to -22.2‰ between 1965-2003 AD, suggesting increased terrestrial OC contribution again over the last 50 years. More quantitative estimates of terrestrial OC proportion can be made with a two-endmember mixing model based on TOC-δ^{13}C values (Li et al., 2018; Wu et al., 2018; Zhang et al., 2021). Because the Huanghe POC is mainly (>90%) from the Chinese Loess Plateau (Ren and Shi, 1986; Zhang et al., 1990), a highly uniform wind-blown silt deposits (Xu et al., 2006), it is reasonable to assume that Huanghe POC δ^{13}C endmember is stable over the last 300 years despite the relocation event occurred. The calculations are as following:

$$\delta^{13}C_{sample} = \delta^{13}C_{terrestrial} \times f_{terrestrial} + \delta^{13}C_{marine} \times f_{marine} \quad (4)$$

$$f_{terrestrial} + f_{marine} = 1 \quad (5)$$

By using the Huanghe terrestrial δ^{13}C endmember of -24.0 ± 0.4‰ and marine OC endmember of -20.8 ± 0.8‰, the binary mixing model yields terrestrial contribution of 24% to 45% (**Figure 6E**), with higher average values of 31 and 39% during 1715-1853 AD and 1953-2003 AD, respectively; and a lower average value of 26% during 1865-1940 AD. Furthermore, terrestrial OC content ($OC_{terr.}$) and mass accumulation rate (MAR-$OC_{terr.}$) was calculated for core HH12, which falls in the range of 0.11-0.30% (wt) and 1.3-2.6 g m^{-2} yr^{-1} (**Figure 4A**), respectively. Both $OC_{terr.}$ and MAR-$OC_{terr.}$ records showed lower values during 1865-1953 AD, higher values prior to 1855 AD and after 1955 AD (**Figure 8A**). Taken together, the Huanghe relocation reduced the terrestrial OC burial in site HH12 during 1855-1950 AD.

The third evidence comes from terrestrial *n*-alkanes record. Long-chain *n*-alkanes are major components of higher plant wax (Eglinton and Hamilton, 1967; Eglinton and Eglinton, 2008) and are more resistant to degradation than other classes of OC during lateral transport and deposition processes, therefore have been widely used to trace terrestrial OC in marginal seas (Xing et al., 2011, 2014). The long-chain *n*-alkanes in core HH12 have an obvious odd/even dominance as indicated by CPI values of 2.9-4.4 (**Figure 4C**), confirming the high plant sources of long-chain *n*-alkanes. To be consistent with previous studies in Chinese marginal seas (Xing et al., 2011, 2014), the sum of C_{27}, C_{29}, and C_{31} *n*-alkanes, i.e., Σ (C_{27} + C_{29} + C_{31}), was used to represent terrestrial OC, whose content and MAR showed higher values during 1705-1853 AD compared with 1865-1953 AD (**Figure 8B**). In addition, both records also showed a significant ($p < 0.05$) increase over the last 50 years (**Figure 8B**). In general, the long-chain *n*-alkanes showed similar temporal pattern with that terrestrial OC calculated basing on binary model of TOC-δ^{13}C.

Generally, *n*-alkanes from C_4 grasses have longer chain length than those of trees (Vogts et al., 2009; Zech et al., 2009), therefore average chain length (ACL) of leaf wax *n*-alkane has been used to distinguish vegetation types (Vogts et al., 2009). The calculated ACL of long-chain *n*-alkanes revealed higher values of 29.3-29.6 (average: 29.5) between 1715-1853 AD, a sharp drop to lower values of 28.9-29.3 (average: 29.2) between 1865-1940 AD, and an increase to higher values of 29.4-29.6 (average: 29.5) again

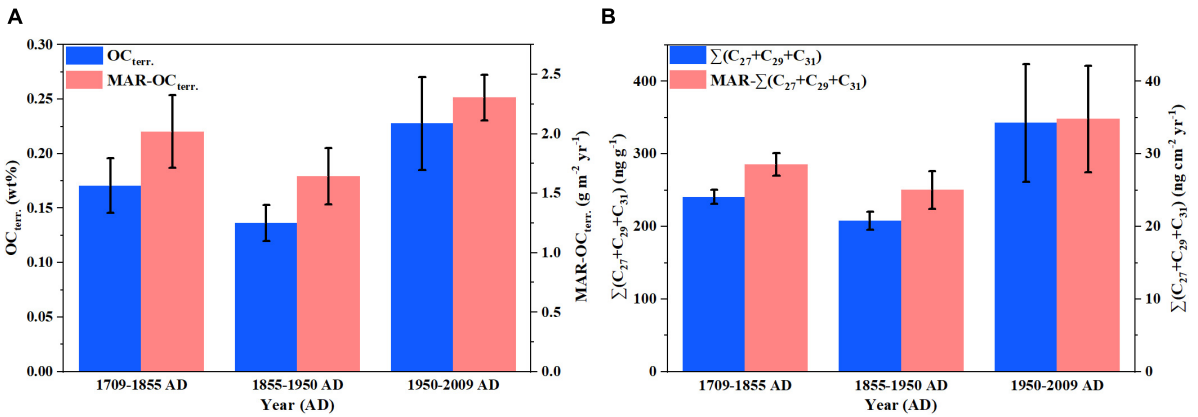

FIGURE 8 | Content and mass accumulation rates (MAR) of terrestrial OC **(A)** and long-chain *n*-alkanes **(B)**, i.e., Σ (C_{27} + C_{29} + C_{31}), from core HH12 during different time intervals. The content and mass accumulation rate of terrestrial OC were calculated using $\delta^{13}C$ binary mixing model. The error bar represents associated 1σ uncertainty. Content of long chain *n*-alkanes was expressed in ng per g dry sediment (ng g^{-1}). According to the *t*-test statistical analyses performed on software package SPSS 22 (IBM), there exist significant differences ($p < 0.05$) of data among the time intervals. Therefore, temporal changes of terrestrial OC and biomarker with respect to the time intervals of 1709-1855 AD, 1855-1950 AD, 1950-2009 AD are significant.

over the last 60 years (**Figure 4D**). However, the variation of ACL could not be explained by changes of plant type over the last 300 years because $\Delta^{14}C$ analysis on *n*-C_{29} and *n*-C_{31} alkanes from the Huanghe river POM reveals radiocarbon ages up to 5380 yr (Tao et al., 2015), indicating that odd number long-chain *n*-alkanes resides for thousands years in soil before being transported into marginal seas. The most possible explanation for the ACL variation in core HH12 is the terrestrial source changes. ACL of long-chain *n*-alkanes from the southern YS surface sediments displayed higher values near the old Huanghe estuary and lower values in the southern YS mud area (Zhang, 2011). The lower ACL values in the CSYSM suggests reduced terrestrial OC contribution from old Huanghe with increased distance from the estuary. By analogy, we proposed that higher ACL values of core HH12 before 1855 AD was the result of higher terrestrial OC contribution from the Huanghe source, and lower values during 1855-1950 AD was the result of reduced terrestrial OC contribution from the Huanghe river due to the extended transport distance. Additional long-chain *n*-alkane measurements on other rivers discharging into the YS are needed to verify this postulation.

Schematic Diagram of Huanghe Relocation on Organic Carbon Burial

Our biogeochemical results document the impact of 1855 AD Huanghe relocation on OC burial in the southern YS. Combined with previous results, we propose a schematic diagram for the connection between this relocation event and OC burial in the southern YS and the ECS (**Figure 9**). In the ∼100 years before and after 1855 AD, the Huanghe runoff and its sediment load was relatively stable (Liu et al., 2020; Wu et al., 2020). When Huanghe emptied into the southern YS during the period 1128-1855 AD, Huanghe sediments were directly transported to the Jiangsu coast, and consequently more fine particles (**Figure 4E**, median grain size from a core 35009 which lies close to core HH12) were transported to the CSYSM. Since clay mineral has higher terrestrial OC loading (Yu et al., 2019b) and favors OC preservation, a combination of these processes resulted in higher terrestrial OC burial in the southern YS (**Figures 8**, **9A**). After 1855 AD, the Huanghe changed its course to discharge into the BS. Extended distance between the modern Huanghe estuary and the southern YS resulted in only a portion of Huanghe derived sediment, 40-60 Mt yr^{-1} (Bi et al., 2011, 2021), and terrestrial OC being transported into the southern YS, *via* the coastal current. In addition, the cut off of fluvial sediment supply to the Jiangsu coast caused the old Huanghe delta to be eroded under the interaction of tidal and coastal currents, which made the particles being transported to the southern YS being coarser. On the other hand, strong hydrodynamic processes resulted in lower OC content of this eroded sediments (Yu et al., 2021). Taken together, the 1855 AD Huanghe relocation dramatically altered terrigenous material sources and amount transported to site HH12, resulting in larger median grain size and lower terrestrial OC flux in the CSYSM.

There also exist different spatial responses of OC burial in the southern YS and the ECS to the 1855 AD Huanghe relocation. Huanghe was the major source of sediment (Millman et al., 1985; Yang et al., 2009) and terrestrial OC to the southwestern SWCIM (Van der Voort et al., 2018; Zhang et al., 2021). Based on published $\delta^{13}C$ of sediment OC, we calculated terrestrial OC contribution for core S05 by using endmembers discussed in section 4.1.2. Compared with core HH12, terrestrial OC contribution in core S05 was higher before 1855 AD and was lower after 1855 AD (**Figure 6F**), suggesting distinct impact of Huanghe relocation on OC in the southern YS and ECS for the following reasons. When the Huanghe discharged into the southern YS before 1855 AD, large amount of Huanghe derived OC could be effectively transported into site S05 in the ECS through strong coastal current along the Jiangsu coast; although site HH12 lies closer to the Huanghe estuary in Jiangsu coast, there was no current that directly transported terrestrial OC to site HH12. In addition, HH12 lies in the

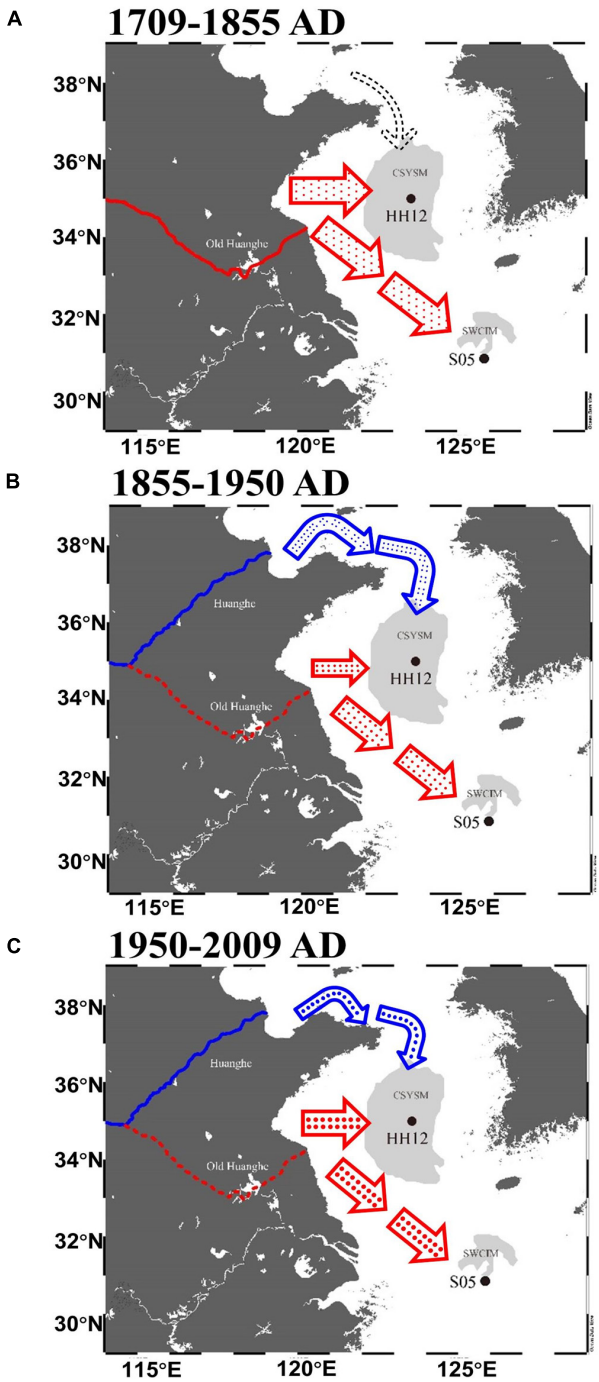

FIGURE 9 | Schematic diagram for Chinese river sourced terrigenous material transports during three-stage changes [**(A)** 1709–1855 AD, **(B)** 1855–1950 AD, **(C)** 1950–2009 AD]. The arrows indicate transport pathways of terrigenous materials; the arrow size indicates the flux of terrigenous material transported; dots in the arrows represents grain size with larger dot indicating coarser sediment and vice versa.

southern YS cold water mass which inhabits efficient transport of coastal material to the CSYSM (Zhong et al., 2020). Therefore, higher terrestrial OC contribution occurred in the SWCIM compared with the CSYSM. After the Huanghe estuary shift into the BS, the distances between Huanghe estuary and sediment sites increased from ∼370 and ∼700 km before 1855 AD to ∼680 and ∼1190 km after 1855 AD for site HH12 and S05, respectively, significantly reducing the content and MAR of terrestrial OC in both southern YS and the ECS. Compared with the southern YS, extended distance significantly reduced terrestrial OC to the ECS either from the modern Huanghe or eroded sediments from the old Huanghe estuary, resulting in lower terrestrial OC contribution in site S05 compared with HH12 (**Figure 9**).

Elevated Terrestrial Organic Carbon Burial in the Southern Yellow Sea After 1950 AD

From 1865 AD to the present, TOC/TN ratio of core HH12 indicated a stable terrestrial OC contribution. Similar patterns have been observed in TOC/TN records of core 35009 (same site as core HH12) in the southern YS and core S05 in the ECS. However, the TOC-$\delta^{13}C$ record of core HH12 showed a significant increase of relative terrestrial OC contribution over the last 50 years (**Figure 6E**), this has been further supported by elevated Σ (C_{27} + C_{29} + C_{31}) values of core HH12 (**Figure 4B**). It should be noted that in the upper centimeters of sediments cores, higher values of OC and biomarker contents may be the result of low degree of degradation toward the core-top even if supply remained constant (Canuel and Martens, 1996; Zimmerman and Canuel, 2000). Since terrestrial OC is more resistant to degradation compared with marine OC, thus positive shift should be observed on $\delta^{13}C$ values in the uppermost centimeters if degradation controls terrestrial OC content and terrestrial vs. marine OC proportions (Zonneveld et al., 2010). However, the negative shift of TOC-$\delta^{13}C$ in core HH12 over the last 50 years does not support this scenario, not consistent with degradation as the primary factor controlling the $\delta^{13}C$. During the past several decades, increases in fertilizer use and sewage discharge led to significant eutrophication in the BH and the YS coastal waters (Tang et al., 2003; Wu et al., 2016), meanwhile, significant decreases of water and sediment load may have also changed the proportion of freshwater phytoplankton derived OC which is characterized by different $\delta^{13}C$ from that of Chinese Loess Plateau soil OC in Huanghe POC. Although these factors may also account for sedimentary TOC-$\delta^{13}C$ changes, MAR-$OC_{terr.}$ record calculated using the $\delta^{13}C$ binary model showed higher values over the last 50 years in core HH12, and this was further supported by elevated MAR of Σ (C_{27} + C_{29} + C_{31}) values (**Figure 4B**). Therefore, we suggest that terrestrial OC transported into the CSYSM increased since 1950s.

The Huanghe sediments were initially deposited in the estuary in the Dongying coast after 1855 AD, then sediments were transported to the southern YS by the Shandong Peninsula Coastal Current which was driven by the East Asian Winter Monsoon (EAWM). Therefore, the terrigenous materials in Chinese marginal seas undergone the "store in summer, transport in winter" process (Hu et al., 2012; Hao et al., 2017). When the EAWM is stronger, more terrestrial sediment along with

terrestrial OC should be transported into the southern YS, and vice versa less for weaker EAWM state. In addition, coarser sediment should be accompanied with stronger EAWM. However, instrument data showed that the wind intensity of EAWM has been weakening since the 1950s (Nakamura et al., 2002; He and Wang, 2012; Liu et al., 2019). Therefore, EAWM driven coastal current is not likely the explanation for increased terrestrial OC in core HH12 and increased grain size in core 35009 (Zhou X. et al., 2014). However, the average Huanghe sediment yield has dropped significantly from 1320 Mt yr^{-1} (Milliman and Meade, 1983) in 1950s AD to 150 Mt yr^{-1} (Wang et al., 2011) during the period 2000-2008 AD, primarily caused by human activities of damming and afforestation (Wang et al., 2011). This significantly reduced the terrestrial OC proportion in BS sediment (core B66, **Figure 6D**). Over the last 40 years, the Huanghe sediment yield to the estuary is not enough to account for sediment transported by coastal currents to the BS and YS, and eroded sediment from the Huanghe delta lobe contributed ∼78% of the Huanghe-borne sediment to the mud deposits in the BS and YS (Bi et al., 2021). This eroded Huanghe derived sediment may become coarser and was further transported into the southern YS mud region through coastal current.

Due to the reduction of southward sediment transport from the BS, eroded sediment from the old Huanghe delta may have increased its proportion and became the main source of sediment into the CSYSM (Yang et al., 2003; Yang and Youn, 2007; Liu et al., 2010; Bian et al., 2013). As showed in **Figure 4D**, the ACL values of long-chain alkanes increased to similar values before 1855 AD, giving further support that eroded sediment from the old Huanghe delta became the dominant terrestrial OC source since 1950 AD. The dike construction along the Jiangsu coast since the 1930s protected subaerial old Huanghe delta from erosion (Liu et al., 2013), but the subaqueous old Huanghe delta erosion increased under the persist strong waves and tidal current (Ren, 1992). Continuous "hydrodynamic sorting effect" on eroded sediments made sediment coarser, leading to the increase of sediment grain size in the CSYSM (**Figures 4E**, **9C**).

On the other hand in the ECS, TOC-$\delta^{13}C$ of core S05 experienced stable values over the last 150 years, thus different spatial patterns of terrestrial OC burial occurred in the southern YS and SWCIM over the last 50 years. The most probable explanation for stable $\delta^{13}C$ in the ESC is that, unlike the southern YS, terrestrial sources for the SWCIM is mainly from the old Huanghe delta and its terrestrial source is not sensitive to the reduction of human induced Huanghe sediment flux since the 1950s (**Figure 9**). Further analyses on grain size, terrestrial biomarker and carbon isotopes on cores collected along the Shandong Peninsula sediment pathway are need to verify this.

Our discussion on mechanisms controlling OC burial in the southern YS over the last 50 years is preliminary and inconclusive, especially the explanation for the increase of terrestrial OC content and MAR under the condition of reduced Huanghe sediment flux (and OC flux), weakened EAWM and lower OC content in eroded sediment from the old Huanghe delta. The OC loadings of sediments from the Korean rivers are one to two factors higher than that of Huanghe (Lee et al., 2013; Yoon et al., 2016; Kang et al., 2019), and Korean river POC-$\delta^{13}C$ is lower than that of Huanghe source (**Figure 5**). Thus, a slightly increase of OC proportion from the Korean rivers, especially the Geum River POC characterized by higher TOC/TN and negative $\delta^{13}C$ ratios (**Figure 5A**), could have led to the increase of terrestrial OC content and a negative shift of TOC-$\delta^{13}C$. Future studies should focus on better constraining the OC sources in the southern YS with measurements of $\delta^{13}C$ and $\Delta^{14}C$ on specific biomarkers, such as long-chain *n*-alkanes and fatty acids for terrestrial OC and short-chain fatty acids for marine OC. This would help to distinguish processes contributing to the decrease of TOC-$\delta^{13}C$ and increase of terrestrial biomarker since the 1950s.

In summary, our study showed that the 1855 AD Huanghe relocation exerted significant effect on sedimentary OC burial flux and source proportions in the southern YS. However, considering the complexity of marginal sea deposition environments, it is not possible to make quantitative assessments for this effect on OC burial for the entire southern YS relying solely on our results. With more detailed studies on this topic in the future, it should be able to obtain a comprehensive picture of the impact of the Huanghe relocation on OC burial in eastern Chinese marginal seas. The Huanghe changed its lower course many times during the Holocene (He et al., 2019), another enlightenment from our study is that river mouth relocation should be taken into consideration to interpret down-core OC record and to distinguish controlling factors for the Holocene. River transport is the major pathway for terrestrial OC to be delivered into marginal seas, relocation of river mouths occurs frequently in the world, especially during the Anthropocene when Anthropogenic interventions become dominant. Our study revealed that river mouth relocation affected terrestrial OC transport processes into the sea, which offers new insights into the processes controlling terrestrial OC burial in continental marginal seas.

CONCLUSION

The $\delta^{13}C$ of sediment OC, TOC/TN molar ratio and the terrestrial lipid biomarker of sediment core HH12 from the southern YS were measured to determine the sources and burial fluxes over the past 300 years. We find that terrestrial OC as well as terrestrial lipid biomarker mass accumulation rates were lower between 1855 and 1950 AD than that prior to 1855 AD. This suggests that the relocation of the Huanghe outlet in 1855 AD reduced the transport of terrestrial OC to the southern YS. The average chain length of *n*-alkanes also decreased significantly suggesting terrestrial OC sources into the southern YS also changed. However, the $\delta^{13}C$ record indicates an increase of the relative terrestrial OC contribution to sedimentary OC after 1950 AD and further evidence comes from the increase of long-chain *n*-alkanes mass accumulation rate. We suggest the most likely explanation is the integrated effect of human induced yield reduction of modern Huanghe sediments, increased contributions from the old Huanghe delta erosion or Korean rivers. These impacts can be evaluated in the future by using the coupled ^{14}C and ^{13}C measurements of lipid biomarkers.

DATA AVAILABILITY STATEMENT

The raw data supporting the conclusions of this article will be made available by the authors, without undue reservation.

AUTHOR CONTRIBUTIONS

MZ, D-WL, and JL designed the study and wrote the manuscript. JL and TG carried out measurement on biomarkers and carbon isotopes. All co-authors provided intellectual input for data interpretation and writing of this manuscript.

FUNDING

This study was supported by the National Natural Science Foundation of China (Grants U1706219, 41876076, and 91958104) and by the Fundamental Research Funds for the Central Universities (Grants 202041007 and 201813029).

ACKNOWLEDGMENTS

We thank the crew of R/V Dongfanghong II of the Ocean University of China for the assistance in sediment coring. This is MCTL (Key Laboratory of Marine Chemistry Theory and Technology) contribution #275.

REFERENCES

Bao, R., van der Voort, T. S., Zhao, M., Guo, X., Montluçon, D. B., McIntyre, C., et al. (2018). Influence of hydrodynamic processes on the fate of sedimentary organic matter on continental margins. *Glob. Biogeochem. Cycle* 32, 1420–1432. doi: 10.1029/2018GB005921

Bauer, J. E., Cai, W.-J., Raymond, P. A., Bianchi, T. S., Hopkinson, C. S., and Regnier, P. A. (2013). The changing carbon cycle of the coastal ocean. *Nature* 504, 61–70. doi: 10.1038/nature12857

Beardsley, R. C., Limeburner, R., Hu, D. X., Le, K. T., Cannon, G. A., and Pashinski, D. J. (1983). "Structure of the changjiang river plume in the east china sea during june 1980," in *Proceedings of International Symposium on Sedimentation on the Continental Shelf, with Special Reference to the East China Sea*.

Bi, N., Wang, H., Wu, X., Saito, Y., Xu, C., and Yang, Z. (2021). Phase change in evolution of the modern huanghe (yellow river) delta: process, pattern, and mechanisms. *Mar. Geol.* 437:106516. doi: 10.1016/j.margeo.2021.106516

Bi, N., Yang, Z., Wang, H., Fan, D., Sun, X., and Lei, K. (2011). Seasonal variation of suspended-sediment transport through the southern bohai strait. *Estuar. Coast. Shelf Sci.* 93, 239–247. doi: 10.1016/j.ecss.2011.03.007

Bian, C., Jiang, W., and Greatbatch, R. J. (2013). An exploratory model study of sediment transport sources and deposits in the bohai sea, yellow sea, and east china sea. *J. Geophys. Res. Oceans* 118, 5908–5923. doi: 10.1002/2013JC009116

Blair, N. E., and Aller, R. C. (2012). The fate of terrestrial organic carbon in the marine environment. *Annu. Rev. Mar. Sci.* 4, 401–423. doi: 10.1146/annurev-marine-120709-142717

Burdige, D. J. (2005). Burial of terrestrial organic matter in marine sediments: a re-assessment. *Glob. Biogeochem. Cycle* 19:GB4011. doi: 10.1029/2004GB002368

Calvert, S. E. (2004). Beware intercepts: interpreting compositional ratios in multi-component sediments and sedimentary rocks. *Org. Geochem.* 35, 981–987. doi: 10.1016/j.orggeochem.2004.03.001

Canuel, E. A., and Martens, C. S. (1996). Reactivity of recently deposited organic matter: degradation of lipid compounds near the sediment-water interface. *Geochim. Cosmochim. Acta* 60, 1793–1806. doi: 10.1016/0016-7037(96)00045-2

Eglinton, G., and Hamilton, R. J. (1967). Leaf epicuticular waxes. *Science* 156, 1322–1335. doi: 10.1126/science.156.3780.1322

Eglinton, T. I., and Eglinton, G. (2008). Molecular proxies for paleoclimatology. *Earth Planet. Sci. Lett.* 275, 1–16. doi: 10.1016/j.epsl.2008.07.012

Fan, Y., Fan, D.-J., Zheng, S.-W., Long, H.-Y., Zhang, X.-L., and Tian, Y. (2019). The benthic foraminifera assemblages responds to relocation of yellow river in 1855 in south yellow sea. *J. Ocean Univ.* 49, 101–109. doi: 10.16441/j.cnki.hdxb.20180330

Fan, Y., Lan, J., Zhao, Z., and Zhao, M. (2014). Sedimentary records of hydroxylated and methoxylated polybrominated diphenyl ethers in the southern yellow sea. *Mar. Pollut. Bull.* 84, 366–372. doi: 10.1016/j.marpolbul.2014.05.035

Galy, V., Peucker-Ehrenbrink, B., and Eglinton, T. (2015). Global carbon export from the terrestrial biosphere controlled by erosion. *Nature* 521, 204–207. doi: 10.1038/nature14400

Goñi, M. A., Ruttenberg, K. C., and Eglienton, T. I. (1998). A reassessment of the sources and importance of land-derived organic matter in surface sediments from the gulf of mexico. *Geochim. Cosmochim. Acta* 62, 3055–3075. doi: 10.1016/S0016-7037(98)00217-8

Hao, T., Liu, X., Ogg, J., Liang, Z., Xiang, R., Zhang, X., et al. (2017). Intensified episodes of east asian winter monsoon during the middle through late holocene driven by north atlantic cooling events: high-resolution lignin records from the south yellow sea, china. *Earth Planet. Sci. Lett.* 479, 144–155. doi: 10.1016/j.epsl.2017.09.031

He, L., Xue, C., Ye, S., Amorosi, A., Yuan, H., Yang, S., et al. (2019). New evidence on the spatial-temporal distribution of superlobes in the yellow river delta complex. *Quat. Sci. Rev.* 214, 117–138. doi: 10.1016/j.quascirev.2019.05.003

He, S., and Wang, H. (2012). An integrated east asian winter monsoon index and its international variability. *Chinese J. Atmospheric Sci.* 36, 523–538.

Hedges, J. I., Keil, R. G., and Benner, R. (1997). What happens to terrestrial organic matter in the ocean? *Org. Geochem.* 27, 195–212. doi: 10.1016/s0146-6380(97)00066-1

Hu, B. Q., Yang, Z. S., Zhao, M. X., Saito, Y., Fan, D. J., and Wang, L. B. (2012). Grain size records reveal variability of the east asian winter monsoon since the middle holocene in the central yellow sea mud area, china. *Sci. China Earth Sci.* 55, 1656–1668. doi: 10.1007/s11430-012-4447-7

Huh, C.-A., Chen, W., Hsu, F.-H., Su, C.-C., Chiu, J.-K., Lin, S., et al. (2011). Modern (<100 years) sedimentation in the taiwan strait: rates and source-to-sink pathways elucidated from radionuclides and particle size distribution. *Cont. Shelf Res.* 31, 47–63. doi: 10.1016/j.csr.2010.11.002

Huh, C.-A., and Su, C.-C. (1999). Sedimentation dynamics in the east china sea elucidated from 210Pb, 137Cs and 239,240Pu. *Mar. Geol.* 160, 183–196. doi: 10.1016/S0025-3227(99)00020-1

Jiao, N., Liang, Y., Zhang, Y., Liu, J., Zhang, Y., Zhang, R., et al. (2018). Carbon pools and fluxes in the china seas and adjacent oceans. *Sci. China Earth Sci.* 61, 1535–1563. doi: 10.1007/s11430-018-9190-x

Kang, S., Kim, J.-H., Kim, D., Song, H., Ryu, J.-S., Ock, G., et al. (2019). Temporal variation in riverine organic carbon concentrations and fluxes in two contrasting estuary systems: geum and seomjin, south korea. *Environ. Int.* 133:105126. doi: 10.1016/j.envint.2019.105126

Kao, S.-J., Hilton, R. G., Selvaraj, K., Dai, M., Zehetner, F., Huang, J.-C., et al. (2014). Preservation of terrestrial organic carbon in marine sediments offshore taiwan: mountain building and atmospheric carbon dioxide sequestration. *Earth Surf. Dyn.* 2, 127–139. doi: 10.5194/esurf-2-127-2014

Lamb, A. L., Wilson, G. P., and Leng, M. J. (2006). A review of coastal palaeoclimate and relative sea-level reconstructions using δ13C and C/N ratios in organic material. *Earth Sci. Rev.* 75, 29–57. doi: 10.1016/j.earscirev.2005.10.003

Lee, Y.-J., Jeong, B.-K., Shin, Y.-S., Kim, S.-H., and Shin, K.-H. (2013). Determination of the origin of particulate organic matter at the estuary of youngsan river using stable isotope ratios (δ13C, δ15N). *Korean J. Ecol. Environ.* 46, 175–184. doi: 10.11614/KSL.2013.46.2.175

Li, D., Zhao, M., and Chen, M.-T. (2014). East asian winter monsoon controlling phytoplankton productivity and community structure changes

in the southeastern south china sea over the last 185 kyr. *Palaeogeogr. Palaeoclimatol. Palaeoecol.* 414, 233–242. doi: 10.1016/j.palaeo.2014.09.003

Li, D.-W., Chang, Y.-P., Li, Q., Zheng, L., Ding, X., and Kao, S.-J. (2018). Effect of sea-level on organic carbon preservation in the okinawa trough over the last 91?kyr. *Mar. Geol.* 399, 148–157. doi: 10.1016/j.margeo.2018.02.013

Li, D.-W., Yu, M., Jia, Y., Steinke, S., Li, L., Xiang, R., et al. (2021). Gradually cooling of the yellow sea warm current driven by tropical pacific subsurface water temperature changes over the past 5 kyr. *Geophys. Res. Lett.* 48:e2021GL093534. doi: 10.1029/2021GL093534

Li, G., Li, P., Liu, Y., Qiao, L., Ma, Y., Xu, J., et al. (2014). Sedimentary system response to the global sea level change in the east china seas since the last glacial maximum. *Earth Sci. Rev.* 139, 390–405. doi: 10.1016/j.earscirev.2014.09.007

Li, X., Bianchi, T. S., Allison, M. A., Chapman, P., Mitra, S., Zhang, Z., et al. (2012). Composition, abundance and age of total organic carbon in surface sediments from the inner shelf of the east china sea. *Mar. Chem.* 145-147, 37–52. doi: 10.1016/j.marchem.2012.10.001

Liao, Y.-J., Fan, D.-J., Liu, M., Wang, W.-W., Zhao, Q.-M., and Chen, B. (2015). Sedimentary records correspond to relocation of huanghe river in bohai sea. *Period. Ocean Univ.* 45, 88–100. doi: 10.16441/j.cnki.hdxb.20140055

Lim, D., Kim, J., Xu, Z., Jung, H., Yoo, D.-G., Choi, M., et al. (2020). Quantitative reconstruction of holocene sediment source variations in the yellow and northern east china seas and their forcings. *Mar. Geol.* 430:106345. doi: 10.1016/j.margeo.2020.106345

Lim, D. I., Choi, J. Y., Jung, H. S., Rho, K. C., and Ahn, K. S. (2007). Recent sediment accumulation and origin of shelf mud deposits in the yellow and east china seas. *Prog. Oceanogr.* 73, 145–159. doi: 10.1016/j.pocean.2007.02.004

Lin, X., Yang, J., Guo, J., Zhang, Z., Yin, Y., Song, X., et al. (2011). An asymmetric upwind flow, yellow sea warm current: 1. new observations in the western yellow sea. *J. Geophys. Res.* 116:C04026. doi: 10.1029/2010JC006513

Liu, J., Kong, X., Saito, Y., Liu, J. P., Yang, Z., and Wen, C. (2013). Subaqueous deltaic formation of the old yellow river (AD 1128–1855) on the western south yellow sea. *Mar. Geol.* 344, 19–33. doi: 10.1016/j.margeo.2013.07.003

Liu, J., Saito, Y., Kong, X., Wang, H., Wen, C., Yang, Z., et al. (2010). Delta development and channel incision during marine isotope stages 3 and 2 in the western south yellow sea. *Mar. Geol.* 278, 54–76. doi: 10.1016/j.margeo.2010.09.003

Liu, J. P., Xu, K. H., Li, A. C., Milliman, J. D., Velozzi, D. M., Xiao, S. B., et al. (2007). Flux and fate of yangtze river sediment delivered to the east china sea. *Geomorphology* 85, 208–224. doi: 10.1016/j.geomorph.2006.03.023

Liu, W., Feng, X., Ning, Y., Zhang, Q., Cao, Y., and An, Z. (2005). δ13C variation of C3 and C4 plants across an asian monsoon rainfall gradient in arid northwestern china. *Glob. Change Biol.* 11, 1094–1000. doi: 10.1111/j.1365-2486.2005.00969.x

Liu, X., Hu, L., Wu, X., Wang, Y., and Xu, J. (2019). Evolution of the mud patch in the north yellow sea and its response to climate change in the past 160 years. *Anthropocene Coasts* 2, 193–208. doi: 10.1139/anc-2018-0017

Liu, Y., Song, H., An, Z., Sun, C., Trouet, V., Cai, Q., et al. (2020). Recent anthropogenic curtailing of yellow river runoff and sediment load is unprecedented over the past 500 y. *Proc. Natl. Acad. Sci. U.S.A.* 117, 18251–18257. doi: 10.1073/pnas.1922349117

Lu, X. (2004). Application of the weibull extrapolation to 137Cs geochronology in tokyo bay and ise bay, japan. *J. Environ. Radioact.* 73, 169–181. doi: 10.1016/j.jenvrad.2003.08.009

Lu, X., and Matsumoto, E. (2005). Recent sedimentation rates derived from 210Pb and 137Cs methods in ise bay, japan. *Estuar. Coast. Shelf Sci.* 65, 83–93. doi: 10.1016/j.ecss.2005.05.009

Meyers, P. A. (1997). Organic geochemical proxies of paleoceanographic, paleolimnologic, and paleoclimatic processes. *Org. Geochem.* 27, 213–250. doi: 10.1016/S0146-6380(97)00049-1

Meyers, P. A., and Ishiwatari, R. (1993). Lacustrine organic geochemistry—an overview of indicators of organic matter sources and diagenesis in lake sediments. *Org. Geochem.* 20, 867–900. doi: 10.1016/0146-6380(93)90100-P

Millman, J. D., Beardsley, R. C., Yang, Z.-S., and Limeburner, R. (1985). Modern Huanghe-derived muds on the outer shelf of the east china sea: identification and potential transport mechanisms. *Cont. Shelf Res.* 4, 175–188. doi: 10.1016/0278-4343(85)90028-7

Milliman, J. D., and Meade, R. H. (1983). World-wide delivery of river sediment to the oceans. *J. Geol.* 91, 1–21. doi: 10.1086/628741

Müller, P. J. (1977). C/N ratios in pacific deep-sea sediments: effect of inorganic ammonium and organic nitrogen compounds sorbed by clays. *Geochim. Cosmochim. Acta* 41, 765–776. doi: 10.1016/0016-7037(77)90047-3

Nakamura, H., Izumi, T., and Sampe, T. (2002). Interannual and decadal modulations recently observed in the pacific storm track activity and east asian winter monsoon. *J. Clim.* 15, 1855–1874. doi: 10.1175/1520-04422002015<1855:iadmro<2.0.co;2

O'Leary, M. H. (1988). Carbon isotopes in photosynthesis. *BioScience* 38, 328–336. doi: 10.2307/1310735

Qiao, S., Shi, X., Wang, G., Zhou, L., Hu, B., Hu, L., et al. (2017). Sediment accumulation and budget in the bohai sea, yellow sea and east china sea. *Mar. Geol.* 390, 270–281. doi: 10.1016/j.margeo.2017.06.004

Redfield, A. C., Ketchum, B. H., and Richards, F. A. (1963). *The Influence of Organisms on the Composition of Seawater*. Wiley, NY: Wiley Interscience,

Ren, M. (1992). Human impact on coastal landform and sedimentation. *Geo J.* 28, 443–448. doi: 10.1007/BF00273113

Ren, M.-E., and Shi, Y.-L. (1986). Sediment discharge of the yellow river (china) and its effect on the sedimentation of the bohai and the yellow sea. *Cont. Shelf Res.* 6, 785–810. doi: 10.1016/0278-4343(86)90037-3

Ritchie, J. C., and McHenry, J. R. (1990). Application of radioactive fallout cesium-137 for measuring soil erosion and sediment accumulation rates and patterns: a review. *J. Environ. Qual.* 19, 215–233. doi: 10.2134/jeq1990.00472425001900020006x

Schubert, C. J., and Calvert, S. E. (2001). Nitrogen and carbon isotopic composition of marine and terrestrial organic matter in arctic ocean sediments: implications for nutrient utilization and organic matter composition. *Deep Sea Res. I* 48, 789–810. doi: 10.1016/S0967-0637(00)00069-8

Smith, J. N. (2001). Why should we believe 210Pb sediment geochronologies? *J. Environ. Radioact.* 55, 121–123. doi: 10.1016/S0265-931X(00)00152-1

Sun, X., Fan, D., Cheng, P., Hu, L., Sun, X., Guo, Z., et al. (2021). Source, transport and fate of terrestrial organic carbon from yangtze river during a large flood event: insights from multiple-isotopes (δ13C, δ15N, Δ14C) and geochemical tracers. *Geochim. Cosmochim. Acta* 308, 217–236. doi: 10.1016/j.gca.2021.06.004

Tang, Q., Jin, X., Wang, J., Zhuang, Z., Cui, Y., and Meng, T. (2003). Decadal-scale variations of ecosystem productivity and control mechanisms in the bohai sea. *Fish. Oceanogr.* 12, 223–233. doi: 10.1046/j.1365-2419.2003.00251.x

Tao, S., Eglinton, T. I., Montluçon, D. B., McIntyre, C., and Zhao, M. (2015). Pre-aged soil organic carbon as a major component of the yellow river suspended load: regional significance and global relevance. *Earth Planet. Sci. Lett.* 414, 77–86. doi: 10.1016/j.epsl.2015.01.004

Van der Voort, T. S., Mannu, U., Blattmann, T. M., Bao, R., Zhao, M., and Eglinton, T. I. (2018). Deconvolving the fate of carbon in coastal sediments. *Geophys. Res. Lett.* 45, 4134–4142. doi: 10.1029/2018GL077009

Vogts, A., Moossen, H., Rommerskirchen, F., and Rullkötter, J. (2009). Distribution patterns and stable carbon isotopic composition of alkanes and alkan-1-ols from plant waxes of african rain forest and savanna C3 species. *Org. Geochem.* 40, 1037–1054. doi: 10.1016/j.orggeochem.2009.07.011

Wang, H., Saito, Y., Zhang, Y., Bi, N., Sun, X., and Yang, Z. (2011). Recent changes of sediment flux to the western pacific ocean from major rivers in east and southeast asia. *Earth Sci. Rev.* 108, 80–100. doi: 10.1016/j.earscirev.2011.06.003

Wang, Z., Li, L., Chen, D., Xu, K., Wei, T., Gao, J., et al. (2007). Plume front and suspended sediment dispersal off the yangtze (changjiang) river mouth, china during non-flood season. *Estuar. Coast. Shelf Sci.* 71, 60–67. doi: 10.1016/j.ecss.2006.08.009

Wu, X., Duan, H., Bi, N., Yuan, P., Wang, A., and Wang, H. (2016). Interannual and seasonal variation of chlorophyll-a off the yellow river mouth (1997–2012): dominance of river inputs and coastal dynamics. *Estuar. Coast. Shelf Sci.* 183, 402–412. doi: 10.1016/j.ecss.2016.08.038

Wu, X., Wang, H., Bi, N., Saito, Y., Xu, J., Zhang, Y., et al. (2020). Climate and human battle for dominance over the yellow river's sediment discharge: from the mid-holocene to the anthropocene. *Mar. Geol.* 425:106188. doi: 10.1016/j.margeo.2020.106188

Wu, Y., Eglinton, T. I., Zhang, J., and Montlucon, D. B. (2018). Spatiotemporal variation of the quality, origin, and age of particulate organic matter transported by the yangtze river (changjiang). *J. Geophys. Res. Biogeosci.* 123, 2908–2921. doi: 10.1029/2017JG004285

Xiao, R., Wu, X., Du, J., Deng, B., and Xing, L. (2020). Impacts of anthropogenic forcing on source variability of sedimentary organic matter in the yellow river estuary over the past 60 years. *Mar. Pollut. Bull.* 151:110818. doi: 10.1016/j.marpolbul.2019.110818

Xing, L., Tao, S., Zhang, H., Liu, Y., Yu, Z., and Zhao, M. (2011). Distributions and origins of lipid biomarkers in surface sediments from the southern yellow sea. *Appl. Geochem.* 26, 1584–1593. doi: 10.1016/j.apgeochem.2011.06.024

Xing, L., Zhao, M., Gao, W., Wang, F., Zhang, H., Li, L., et al. (2014). Multiple proxy estimates of source and spatial variation in organic matter in surface sediments from the southern yellow sea. *Org. Geochem.* 76, 72–81. doi: 10.1016/j.orggeochem.2014.07.005

Xu, J., Yang, J., and Yan, Y. (2006). Erosion and sediment yields as influenced by coupled eolian and fluvial processes: the yellow river, china. *Geomorphology* 73, 1–15. doi: 10.1016/j.geomorph.2005.03.012

Yang, S., Bi, L., Li, C., Wang, Z., and Dou, Y. (2016). Major sinks of the changjiang (yangtze river)-derived sediments in the east china sea during the late quaternary. *Geol. Soc. Lond. Spec. Publ.* 429, 137–152. doi: 10.1144/SP429.6

Yang, S., and Youn, J.-S. (2007). Geochemical compositions and provenance discrimination of the central south yellow sea sediments. *Mar. Geol.* 243, 229–241. doi: 10.1016/j.margeo.2007.05.001

Yang, S. Y., Jung, H. S., Lim, D. I., and Li, C. X. (2003). A review on the provenance discrimination of sediments in the yellow sea. *Earth Sci. Rev.* 63, 93–120. doi: 10.1016/S0012-8252(03)00033-3

Yang, W., Chen, M., Li, G., Cao, J., Guo, Z., Ma, Q., et al. (2009). Relocation of the yellow river as revealed by sedimentary isotopic and elemental signals in the east china sea. *Mar. Pollut. Bull.* 58, 923–927. doi: 10.1016/j.marpolbul.2009.03.019

Yoon, S.-H., Kim, J.-H., Yi, H.-I., Yamamoto, M., Gal, J.-K., Kang, S., et al. (2016). Source, composition and reactivity of sedimentary organic carbon in the river-dominated marginal seas: a study of the eastern yellow sea (the northwestern pacific). *Cont. Shelf Res.* 125, 114–126. doi: 10.1016/j.csr.2016.07.010

Yu, M., Eglinton, T. I., Haghipour, N., Montlucon, D. B., Wacker, L., Hou, P., et al. (2019a). Impacts of natural and human-induced hydrological variability on particulate organic carbon dynamics in the yellow river. *Environ. Sci. Technol.* 53, 1119–1129. doi: 10.1021/acs.est.8b04705

Yu, M., Eglinton, T. I., Haghipour, N., Montluçon, D. B., Wacker, L., Wang, Z., et al. (2019b). Molecular isotopic insights into hydrodynamic controls on fluvial suspended particulate organic matter transport. *Geochim. Cosmochim. Acta* 262, 78–91. doi: 10.1016/j.gca.2019.07.040

Yu, M., Eglinton, T. I., Haghipour, N., Montluçon, D. B., Wacker, L., Hou, P., et al. (2021). Contrasting fates of terrestrial organic carbon pools in marginal sea sediments. *Geochim. Cosmochim. Acta* 309, 16–30. doi: 10.1016/j.gca.2021.06.018

Zang, J., Tang, Y., Zou, E., and Lie, H.-J. (2003). Analysis of yellow sea circulation. *Chin. Sci. Bull.* 48, 12–20. doi: 10.1007/BF02900935

Zech, M., Buggle, B., Leiber, K., Markovic, S., Glaser, B., Hambach, U., et al. (2009). Reconstructing quaternary vegetation history in the carpathian basin, SE-europe, using n-alkane biomarkers as molecular fossils: problems and possible solutions, potential and limitations. *J. Quat. Sci.* 58, 148–155. doi: 10.3285/eg.58.2.03

Zhang, H., Li, D.-W., Sachs, J. P., Yuan, Z., Wang, Z., Su, C., et al. (2021). Hydrodynamic processes and source changes caused elevated 14C ages of organic carbon in the east china sea over the last 14.3 kyr. *Geochim. Cosmochim. Acta* 304, 347–363. doi: 10.1016/j.gca.2021.04.015

Zhang, J., Huang, W. W., and Shi, M. C. (1990). Huanghe (yellow river) and its estuary: sediment origin, transport and deposition. *J. Hydrol.* 120, 203–223. doi: 10.1016/0022-1694(90)90150-V

Zhang, R. (1984). Land-forming history of the huanghe river delta and coastal plain of north jiangsu. *Acta Geogr. Sin.* 39, 173–184.

Zhang, Y. (2011). *The Composition And Distribution Of N-Alkanes In Surface Sediments From The South Yellow Sea And Their Potential As Organic Matter Source Indicators Ph. D, Thesis*. Ocean University of China.

Zhao, B., Yao, P., Bianchi, T. S., and Yu, Z. G. (2021). Controls on organic carbon burial in the eastern china marginal seas: a regional synthesis. *Glob. Biogeochem. Cycle* 35:e2020GB006608. doi: 10.1029/2020GB006608

Zhong, Y., Qiao, L., Song, D., Ding, Y., Xu, J., Xue, W., et al. (2020). Impact of cold water mass on suspended sediment transport in the south yellow sea. *Mar. Geol.* 428:106244. doi: 10.1016/j.margeo.2020.106244

Zhou, L., Liu, J., Saito, Y., Zhang, Z., Chu, H., and Hu, G. (2014). Coastal erosion as a major sediment supplier to continental shelves: example from the abandoned old huanghe (yellow river) delta. *Cont. Shelf Res.* 82, 43–59. doi: 10.1016/j.csr.2014.03.015

Zhou, X., Jia, N., Cheng, W., Wang, Y., and Sun, L. (2013). Relocation of the yellow river estuary in 1855 AD recorded in the sediment core from the northern yellow sea. *J. Ocean Univ.* 12, 624–628. doi: 10.1007/s11802-013-2199-4

Zhou, X., Sun, L., Huang, W., Liu, Y., Jia, N., and Cheng, W. (2014). Relationship between magnetic susceptibility and grain size of sediments in the china seas and its implications. *Cont. Shelf Res.* 72, 131–137. doi: 10.1016/j.csr.2013.07.011

Zimmerman, A. R., and Canuel, E. A. (2000). A geochemical record of eutrophication and anoxia in chesapeake bay sediments: anthropogenic influence on organic matter composition. *Mar. Chem.* 69, 117–137. doi: 10.1016/S0304-4203(99)00100-0

Zonneveld, K. A. F., Versteegh, G. J. M., Kasten, S., Eglinton, T. I., Emeis, K.-C., Huguet, C., et al. (2010). Selective preservation of organic matter in marine environments; processes and impact on the sedimentary record. *Biogeosciences* 7, 483–511. doi: 10.5194/bg-7-483-2010

Conflict of Interest: The authors declare that the research was conducted in the absence of any commercial or financial relationships that could be construed as a potential conflict of interest.

Publisher's Note: All claims expressed in this article are solely those of the authors and do not necessarily represent those of their affiliated organizations, or those of the publisher, the editors and the reviewers. Any product that may be evaluated in this article, or claim that may be made by its manufacturer, is not guaranteed or endorsed by the publisher.